[Review] doi: 10.3866/PKU.WHXB201802061 www.whxb.pku.edu.cn

Heterogeneous Catalysis of CO_2 Hydrogenation to C_{2+} Products

GAO Yunnan, LIU Shizhen, ZHAO Zhenqing, TAO Hengcong, SUN Zhenyu *
State Key Laboratory of Organic-Inorganic Composites, Beijing University of Chemical Technology, Beijing 100029, P. R. China.

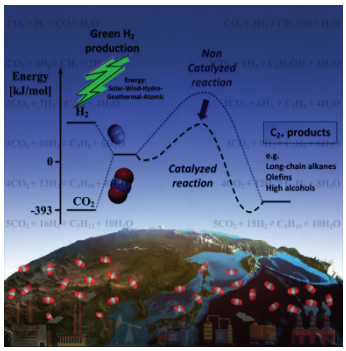

Abstract: The increasing anthropogenic emission of CO_2 leads to global warming, to address which three strategies can be considered: (1) decrease fossil fuel consumption through increased utilization efficiency and lower per capita consumption; (2) replace fossil fuels with renewable energy sources like wind, tidal, solar, and biomass energies; (3) utilize CO_2 efficiently. Despite efforts to reduce energy use and increase the use of carbon-neutral biofuels, it seems that fossil fuels will continue to be a major energy source for the next few decades. Tremendous effort is therefore being focused on developing effective technologies for CO_2 capture and transformation. In particular, the transformation of CO_2 into fuels and chemicals *via* reduction with renewable hydrogen is a promising strategy for mitigating global warming and energy supply problems. The hydrogenation of CO_2, especially to C_{2+} hydrocarbons and oxygenates, has sparked growing interest. The C_{2+} species can be used as entry platform chemicals for existing value chains, thus providing more advantages than C_1 compounds. However, optimizing catalyst design by integrating multifunctionalities for both CO_2 activation and C-C coupling remains an ongoing challenge. Here, we provide a timely review on the recent progress that has been made in the hydrogenation of CO_2 to higher-order alkanes, olefins, and alcohols by various heterogeneous catalysts. The thermodynamics and kinetics, as well as possible reaction pathways for CO_2 hydrogenation, are discussed. The hydrogenation of CO_2 to hydrocarbons usually involves the initial generation of CO *via* a reverse water-gas shift (RWGS) reaction followed by hydrogenation of the CO intermediate. The RWGS reaction proceeds through a redox route and an associative pathway. "CH_x" insertion (carbide-type) and "CO" insertion are two proposed mechanisms for this Fischer-Tropsch-like synthesis. Fe- or Co-based catalysts have been widely used to catalyze the hydrogenation of CO_2 to C_{2+} hydrocarbons *via* the CO intermediate. C_{2+} hydrocarbons can also be obtained by combining CH_3OH synthesis with the methanol-to-hydrocarbon process (MTH). This reaction pathway has been realized over bifunctional systems comprising a CH_3OH synthesis catalyst and an MTH catalyst. Alternatively, CO_2 hydrogenation can occur *via* a RWGS reaction to the CO intermediate, and subsequent formation of higher alcohols from syngas. Higher alcohols (mostly CH_3CH_2OH) have been produced by using a hybrid tandem catalyst. Understanding of the activation mechanism, precise C-C coupling, and synergy control between the two active components requires further research. In the final part, we describe the future challenges and opportunities in heterogeneous catalysis of CO_2 hydrogenation. The combination of calculations (precise theoretical models) and experiments (*in-situ* spectroscopic techniques) will facilitate the design of advanced catalysts to achieve both high CO_2 conversion and C_{2+} product selectivity.

Key Words: CO_2 hydrogenation; Heterogeneous catalysis; C_{2+} species

Received: January 5, 2018; Revised: January 29, 2018; Accepted: January 29, 2018; Published online: February 6, 2018.

*Corresponding author. Email: sunzy@mail.buct.edu.cn.

The project was supported by the State Key Laboratory of Organic-Inorganic Composites, China (oic-201503005), Fundamental Research Funds for the Central Universities, China (buctrc201525) and Beijing National Laboratory for Molecular Sciences, China (BNLMS20160133).
有机无机复合材料国家重点实验室人才培育资助项目(oic-201503005), 北京化工大学引进人才经费(buctrc201525)和北京分子科学国家实验室开放课题基金(BNLMS20160133)资助项目

二氧化碳多相催化加氢制 C_2 及以上烃类和醇的研究进展

高云楠，刘世桢，赵振清，陶亨聪，孙振宇*

北京化工大学，有机无机复合材料国家重点实验室，北京 100029

摘要：通过可再生能源得到的氢气将二氧化碳转化为高附加值的燃料和化学品，对于缓解全球变暖、改善生态环境和解决化石资源日益枯竭的难题具有重要的意义。通过加氢反应合成碳氢化合物，尤其是C_{2+}烃类和含氧化合物愈来愈引起大家的研究兴趣。设计制备兼具二氧化碳活化和碳-碳键耦合的多功能催化剂仍然是一较大的挑战。本文总结了二氧化碳加氢合成长链烷烃、低碳烯烃、高级醇的最新研究进展，探讨了二氧化碳加氢所涉及的相关反应的热力学和动力学、反应机理和反应路径，并对现阶段报道的多相催化剂进行了归纳和分析，最后指出未来在二氧化碳加氢的多相催化过程中所面临的问题和发展方向。

关键词：二氧化碳加氢；多相催化；C_{2+}化合物

中图分类号：O643

1 Introduction

The incessant emission of carbon dioxide (CO_2) into atmosphere resulting from combustion of fossil fuels gives rise to global warming [1]. This situation becomes more intense and unfavorable due to the increase in population, power plant, industries and energy consumption. The CO_2 level is estimated to increase up to 8×10^{-4} (liter per liter air) during this century, and may reach 2×10^{-3} (liter per liter air) by 2300, resulting in further temperature increase and ocean acidification [2]. Fossil fuels likely continue to be a main energy source up to 2050, and possibly beyond. The rapid consumption of fuel fossils also leads to upcoming depletion of natural carbon sources and global energy crisis [3,4]. From these scenarios, conversion of CO_2 to valuable fuels and carbonaceous chemicals appears to be a promising strategy to ameliorate energy shortage and associated environmental problems [5,6]. The efficient utilization of CO_2 as a feedstock of low (or even negative) cost can also create a new and sustainable "CO_2 economy". However, CO_2 is inert and intrinsically stable (ΔG_f^0 = −394.4 kJ·mol^{-1}), thus requiring a substantial input of energy for transformation [~750 kJ·mol^{-1} needed for dissociation of the C=O bond compared with that of C−C (336 kJ·mol^{-1}), C−O (327 kJ·mol^{-1}), and C−H (411 kJ·mol^{-1})].

SUN Zhenyu is currently a full professor in the College of Chemical Engineering at Beijing University of Chemical Technology (China). He completed his Ph.D. in the Institute of Chemistry, Chinese Academy of Sciences in 2006. He did postdoctoral research in Trinity College Dublin (Ireland) from 2006 to 2008, at Ruhr University Bochum (Germany) from 2011 to 2014, and University of Oxford from 2015 to 2016. He has obtained a Humboldt Research Fellowship for Experienced Researchers (Germany). His current research focuses on energy conversion reactions using two-dimensional materials.

Although reduction of CO_2 by using solar energy or electricity has attracted research interest, it is still long R&D necessary for practical implementation. Most of known electrocatalysts [7–10] or photocatalysts [11,12] only show activity for the formation of C_1 species, such as carbon monoxide (CO), methane (CH_4), methanol (CH_3OH), and formic acid (HCOOH). In addition, they usually have unsatisfactory efficiency and/or require the use of sacrificial reducing agents. Transformation of CO_2 by using high-energy hydrogen to yield hydrocarbons and/or oxygenates is one of the most intensively investigated areas [13]. Whether CO_2 conversion by hydrogenation contributes to a net reduction in CO_2 emissions is still a matter of debate, which seems to depend on the function of specific products and processes targeted. Nevertheless, CO_2 hydrogenation could be environmentally appealing to storing energy in chemicals and fuels with low carbon footprint when hydrogen is made from water electrolysis by using renewable or non-fossil resources. Homogeneous [14] and heterogeneous [15] catalysts have been applied to accelerate this slow kinetic process by reducing energy barrier. Homogeneous catalysts exhibit high activity and selectivity in CO_2 hydrogenation, but they suffer from drawbacks of high cost, and difficulty in recovery and regeneration. In contrast, heterogeneous catalysts are more chemically stable, cheaper, and easier to recycle, making them more promising for large-scale application in industry [16,17].

In recent years, heterogeneous catalysis of CO_2 hydrogenation to C_{2+} hydrocarbons (up to C_{15} chain length) and/or oxygenates has garnered increasing research effort [18,19], although this area still remains a grand challenge due to high C−C coupling barrier and the competition of C−C bond formation with the H−H and C−H bond formation. The C_{2+} species can be used as entry platform chemicals for existing value chains, offering more advantages than C_1 compounds.

For example, C_2–C_4 alkanes increase the calorific value of natural gas or biogas through injection into gas-distribution grids. Higher (C_{5+}) alkanes are liquids under ambient conditions, and have high energy densities and compatibility with existing liquid-fuel distribution and end-use infrastructures. Hence, they are attractive precursors of jet fuels. C_2–C_4 light olefins are valuable base chemicals for the production of polymers [20]. Relative to CH_3OH, higher alcohols have been regarded as alternative precursors for short-chain olefins as well as better and cleaner fuels because of their high octane numbers and low emissions of NO_x, ozone, CO, and volatile aromatic vapors after combustion [21].

Many excellent reviews and perspectives on the conversion of CO_2 are available [15,20,22–24]. Nonetheless, most of the reviews focus on the production of C_1 products (e.g., CH_4, CH_3OH and its derivatives) [25–27]. Here we examine how CO_2 hydrogenation occurs to generate higher-value C_{2+} chemicals, particularly long-chain alkanes, olefins and alcohols. Relationships between structure and activity in efficient heterogeneous catalyst design are discussed. A foundational summary for possible reaction pathways is provided. An outlook of future opportunities for conversion of CO_2 into C_{2+} fuels *via* hydrogenation is also described.

2 Mechanistic understanding of CO_2 hydrogenation to C_{2+} species

The reverse water-gas shift (RWGS) reaction [Eq. (1)] is key in CO_2 hydrogenation. This reaction enables transformation of refractory CO_2 into more reactive CO by introducing hydrogen. Such endothermic reaction ($\Delta H_{298\ K}$ = 41.2 kJ·mol^{-1}, $\Delta G_{298\ K}$ = 28.6 kJ·mol^{-1}) is remarkably milder than the production of CO by breaking the C—O bond in CO_2 which requires high temperatures (> 2000 ºC).

$$CO_2 + H_2 \rightleftharpoons CO + H_2O \quad (1)$$

The CO, produced by the RWGS reaction, could be further hydrogenated to hydrocarbons and alcohols [Eqs. (2)–(4)] [28]. It can also be converted back into CO_2 and hydrogen in the presence of water following a water gas shift (WGS) reaction pathway. A direct route from CO_2 to C_{2+} hydrocarbons has been also proposed, which however unlikely plays a major role [29]. Despite this being the case, the direct hydrogenation of CO_2 to CH_4 (Sabatier reaction) is possible [Eq. (5)], which consumes the largest use of hydrogen per CO_2 ($\Delta H_{298\ K}$ = −252.9 kJ·mol^{-1}, $\Delta G_{298\ K}$ = −130.8 kJ·mol^{-1}).

$$nCO + (2n + 1)H_2 \rightleftharpoons C_nH_{2n+2} + nH_2O \quad (2)$$

$$nCO + 2nH_2 \rightleftharpoons C_nH_{2n} + n\ H_2O \quad (3)$$

$$nCO + 2nH_2 \rightleftharpoons C_nH_{2n+1}OH + (n - 1)H_2O \quad (4)$$

where n is the stoichiometric coefficient.

$$CO_2 + 4H_2 \rightleftharpoons CH_4 + 2H_2O \quad (5)$$

Compared with traditional Fischer-Tropsch (FT) synthesis, this two-step reaction requires nearly double amounts of hydrogen and generates more water, a byproduct which may deactivate catalyst and slow down the reaction. The conversion of CO_2 by the RWGS reaction is limited due to relatively low temperatures employed in the second step of FT reaction. Only 13%–23% of CO_2 is converted into CO at temperatures between 220 and 300 °C with a H_2/CO_2 ratio of 3 (stoichiometric ratio for CO_2 hydrogenation to —CH_2—) [30]. The maximum conversion of CO_2 ranges from 10% to 50% at reaction temperatures from 200 to 500 °C.

Calculations by using subroutine RGIBBS along with Soave-Redlich-Kwong model showed that above 550 K, increasing reaction temperature had a detrimental effect on the equilibrium conversion of CO_2 and H_2. C_2 compounds were the major products within the temperature range 350–850 K in a C_1-free system, while the formation of longer chain hydrocarbons was favored with the increase of temperature up to 750 K, in a similar way to increasing reaction pressure (within 1 and 30 bar) based on polymerization FT mechanism. CO_2 equilibrium conversion was promoted by increasing H_2/CO_2 ratio, reaching 100% when the ratio was > 4.2 [31]. However, the H_2/CO_2 ratio was shown to have a marginal effect on the yield of hydrocarbons. It was calculated that the addition or in situ removal of water in the tandem system did not affect the equilibrium conversion of CO_2 or the formation of hydrocarbons. The introduction of CO into a CO_2/H_2 mixture keeping constant CO_x/H_2 molar ratio (1 : 3) enhanced the hydrogen yield into hydrocarbons but had a small effect on CO_2 equilibrium conversion at CO/CO_2 molar ratios less than 0.5 [20]. In the case of higher ratios, the CO_2 equilibrium conversion decreased despite increasing the overall CO_x equilibrium conversion due to the conversion of CO into CO_2 through WGS reaction. We should point out that these theoretical results on reaction conditions for the tandem process need to be further confirmed by experiment.

The formation of C_{2+} hydrocarbons and alcohols, albeit being less likely than that of CH_4, is more thermodynamically favorable than that of CH_3OH at low temperatures (Fig. 1a). Zhang and co-workers performed a thermodynamic study, and investigated the ΔG for CO and different hydrocarbons as a function of reaction temperature (Fig. 1b). The variation of temperature was observed to have the minimum effect on the generation of CH_4. At temperatures below about 300 °C (ΔG < 0 for olefins), increasing temperature favored the yield of olefins in the equilibrium products. For the synthesis of C_2–C_4 olefins at CO_2 conversion of 72.8%–74.5%, optimal reaction temperatures were proposed to be in the range 300–400 °C, pressures in the range 2.0–3.0 MPa, and H_2/CO_2 feed gas molar ratio of 3 [32].

3 Possible reaction pathways

3.1 Synthesis of alkanes and olefins

3.1.1 CO_2 hydrogenation *via* CO intermediate

The hydrogenation of CO_2 to hydrocarbons usually involves the initial generation of CO *via* a RWGS reaction. Two important reaction mechanisms on the RWGS reaction have

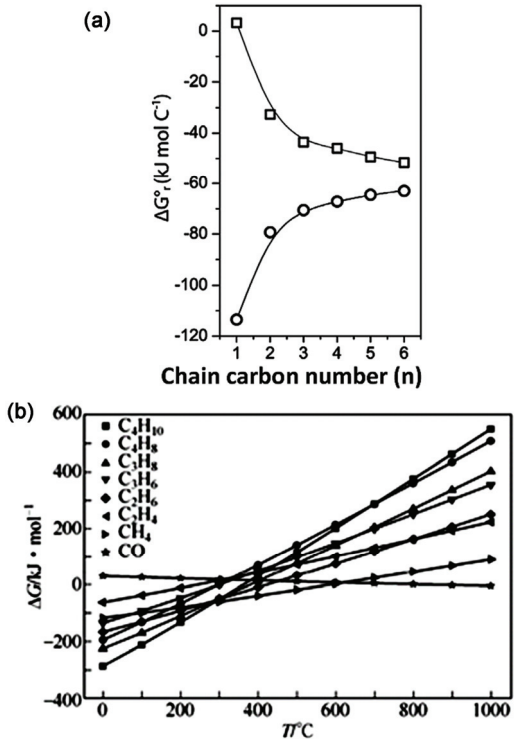

Fig. 1 (a) Evolution of the standard Gibbs reaction free energy for the hydrogenation of CO_2 into *n*-alkanes (○) and terminal *n*-alcohols (□) [20]. (b) Effect of reaction temperature on Gibbs free energy of CO_2 hydrogenation to hydrocarbons and oxygenates [32].

Fig. (a) Reproduced with permission from © 2017 WILEY-VCH Verlag GmbH & Co. KGaA, Weinheim.

been put forth, namely a redox route and an associative pathway. In the redox mechanism, CO_2 is adsorbed and activated on reduced metals or metal oxides to form CO. Hydrogen acts as a reductant, and does not participate in the formation of intermediates in the RWGS reaction. This redox mechanism has been confirmed by XPS analysis of the oxidation states of Pt/TiO_2 catalyst [33]. The associative mechanism is related with the decomposition of intermediates such as surface formate, carbonate, or carboxyl species that are derived from the association of hydrogen with CO_2. The type of intermediate depends on reaction conditions and the catalyst used [34].

In the following FT reaction, formed CO reacts with unconverted H_2. However, the pathway of chain growth in F-T synthesis remains controversial. "CH_x" insertion (carbide type) [35] and "CO" insertion [36] are two proposed mechanisms. The former assumes CO activation either by direct reaction with chemisorbed hydrogen or H-assisted pathway possibly via formyl (HCO^*) and formaldehyde (H_2CO^*) or hydroxymethylene ($HCOH^*$) species to form surface CH_x^* monomer (Fig. 2). The direct CO activation removes O^* from CO_2, while the H-assisted CO dissociation forms H_2O exclusively. The H-assisted route is likely a predominant kinetically-relevant step on Co catalysts as confirmed by experimental measurements and DFT calculations [37].

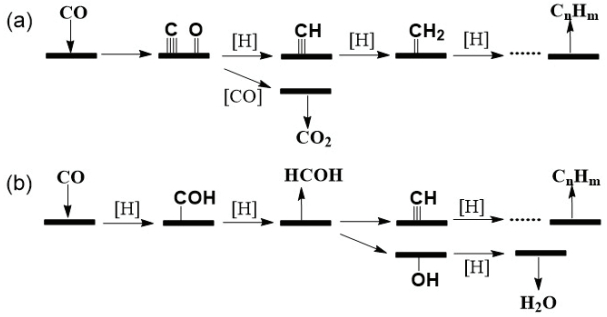

Fig. 2 Possible pathways for the formation of hydrocarbons from CO [37]: (a) direct CO activation pathway on Fe catalysts, and (b) H-assisted pathway on Co catalysts.

Adapted from Elsevier publisher.

In the CO insertion route, RCH_x^* species are speculated to couple with CO^* to form RCH_2CO^* facilitated by surface OH groups, which is followed by deoxyhydrogenation of the oxygen intermediate [36]. Chemical transient [38] and isotope labeling [39] studies have provided support for such CO insertion mechanism. It is clear that CO activation is key to both carbide and CO insertion mechanisms. An Anderson-Schulz-Flory (ASF) model has been developed to estimate chain-growth probability of FT reaction [Eq. (6)] assuming that the probability is independent on the chain length of hydrocarbons.

$$W_n = (\ln^2\alpha)n\alpha^n \quad (6)$$

where W_n represents the weight proportion of products with n carbon atoms in their chain, α stands for the chain-growth probability, and n is the number of carbon atoms. It has been predicted that the fraction of C_5–C_{15} reaches a maximum of 60% at $\alpha = 0.8$. Deviations from the ASF model were observed on Co-based catalysts. This is due to the possibility that CO_2 conversion took place through a separate methanation pathway rather than *via* F-T synthesis. Nevertheless, the α parameter in liquid hydrocarbon products provides a suitable basis for comparison of various product distributions [40].

3.1.2 CO_2 hydrogenation *via* methanol intermediate

C_{2+} hydrocarbons can also be obtained through an initial formation of CH_3OH [Eq. (7), $\Delta H_{298\ K} = -49.5$ kJ·mol^{-1}] followed by its subsequent transformation.

$$CO_2 + 3H_2 \rightleftharpoons CH_3OH + H_2O \quad (7)$$

This reaction pathway has been recognized over bifunctional systems comprising a methanol synthesis catalyst and a methanol-to-hydrocarbon (MTH) catalyst. In a recent study [41], CH_xO species (mainly surface CH_3O^*, CHO^* species, and gas-phase CH_3OH) were found to be generated *via* CO_2 hydrogenation on ZnZrO. These derived CH_xO species migrated into a Zn-modified SAPO-34 zeolite to convert into lower olefins (Fig. 3).

Two reaction mechanisms for CH_3OH formation have been proposed including a formate route and a RWGS pathway. In the formate route, CO_2 is hydrogenated step by step to CH_3OH directly. Whilst in the RWGS pathway, CO_2 is firstly reduced to CO at a metal-support interface, and then consecutively

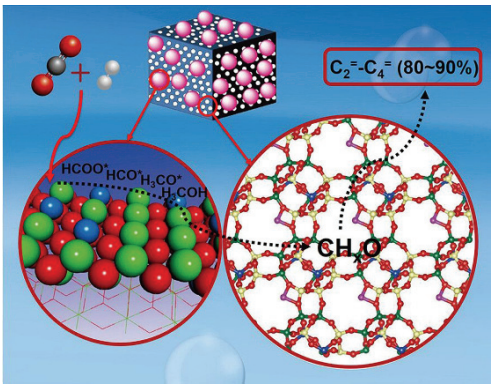

Fig. 3 Schematic of CO_2 hydrogenation reaction mechanism on ZnZrO/SAPO [41].

Reproduced with permission from © 2017 American Chemical Society.

hydrogenated to CH_3OH. CO are released in this process as well, that is why CO is always associated with CH_3OH production.

The MTH process over zeolite catalysts, was first discovered by Mobil Research Laboratories in 1976 [42]. Medium-pore zeolites were reported to produce C_5–C_{11} hydrocarbons, whereas small-pore molecular sieves generated C_2–C_4 hydrocarbons. The distribution of hydrocarbon products is affected by the structure and acidity of zeolite. Possible mechanistic proposals involve oxonium ylide mechanism, carbine mechanism, carbocationic mechanism, free radical mechanism, hydrocarbon pool mechanism, *etc.* [22].

3.2 Synthesis of high alcohols

CO_2 hydrogenation can proceed through a RWGS reaction to CO intermediate, and subsequent the formation of high alcohols from syngas [43,44]. Na in association with the carbide form of cobalt was speculated to enhance the production of ethanol from CO through a CO insertion mechanism, as illustrated in Fig. 4a [45]. Whilst on iron catalysts, CO was hypothesized to dissociate, forming adsorbed oxygen (O_{ad}), which reacted with adsorbed hydrogen, to produce chemisorbed OH (OH_{ad}). The OH_{ad} then reacted with hydrocarbon species such as alkylidenes (R—CH_2—CH=) to yield ethanol, as shown in Fig. 4b [46].

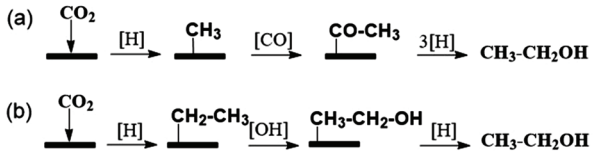

Fig. 4 Proposed pathways for the formation of ethanol over (a) Na-doped Co catalysts [45], and (b) Fe/NCNT catalysts [46].

Adapted from Elsevier publisher.

Alternatively, on $Rh_{10}Se/TiO_2$ catalyst, the evolution of ethanol was suggested to occur from direct CO_2 hydrogenation rather than CO hydrogenation [47]. Specifically, $CH_{x,ads}$ species on Rh reacted with $CO_{y,ads}$ to form acetate, which was further hydrogenated to ethanol on Rh sites.

4 Catalysts of CO_2 hydrogenation to C_{2+} species

4.1 C_{2+} alkanes

The majority of heterogeneous catalysts for CO_2 hydrogenation to alkanes are Fe-, and Co-based catalysts, as

Table 1 Reported catalytic systems for the synthesis of C_{2+} alkanes by CO_2 hydrogenation.

Catalysts	Temperature/°C	Pressure/MPa	CO_2 conversion/%	Alkanes selectivity/%	Ref.
Ce-Mn-Fe/Al_2O_3	290	1.4	38.6	(C_2–C_{5+}) 26.7	48
Fe-Co-K/Al_2O_3	300	1.1	35.8	(C_{2+}) 44.4	49
K-Mn-Fe/Al_2O_3	300	1.8	41.4	(C_2–C_{5+}) 46.1	50
Fe/OCNT	360	2.5	35.2	(C_2–C_5) 29.4	51
Fe/NCNT	360	2.5	25.2	(C_2–C_5) 22.9	52
Co-Na/SiO_2	370	0.1	51.2	(C_2–C_{5+}) 33.1	53
Co-K/SiO_2	370	0.1	47.6	(C_2–C_{5+}) 29.2	53
Co-Na-Mo/SiO_2	370	0.1	43.9	(C_2–C_{5+}) 41.7	53
SiO_2-coating-Fe-K/Al_2O_3	400	3.0	62	(C_2–C_{5+}) 38.0	54
Mn/Fe_2O_3	340	2.0	30	(C_2–C_5) 39.8	55
Na-$ZnFe_2O_4$	340	1.0	34	(C_{5+}) 58.5	56
Fe-K/Al_2O_3	400	3.0	46.5	(C_{5+}) 31.0	57
Fe/CeO_2 particles	390	0.1	26	(C_2–C_{5+}) 5.3	58
Fe/CeO_2 rods	390	0.1	20.6	(C_2–C_{5+}) 6.4	58
Fe/CeO_2 cubes	390	0.1	18.9	(C_2–C_{5+}) 4.7	58
K-CoCu/TiO_2	250	5.0	13	(C_{5+}) 35.1	59
Co-Na-Mo/CeO_2	200	0.1	15.1	(C_2–C_{5+}) 67.2	60
Co-Na-Mo/TiO_2	200	0.1	13.5	(C_2–C_{5+}) 54.8	60
Co-Na-Mo/Al_2O_3	200	0.1	15.4	(C_2–C_{5+}) 67.4	60
Co-Na-Mo/ZrO_2	200	0.1	14.4	(C_2–C_{5+}) 60.3	60
Fe-Cu-K-Si-Al	300	2.0	40.7	(C_2–C_{5+}) 38.5	61

to be continued

continued Table 1

Catalysts	Temperature/°C	Pressure/MPa	CO_2 conversion/%	Alkanes selectivity/%	Ref.
Co/Mo_2C	300	2.0	31	(C_2–C_3) 38	62
Fe_2O_3-CT600	300	1.0	23	(C_{2+}) 29.0	63
$CuFeO_2$	300	1.0	18.1	(C_{5+}) 60.3	64
Fe/SiO_2	370	0.1	36.1	(C_2–C_{5+}) 30.5	65
K-Fe-Co/ZrO_2	400	3.0	43	(C_{2+}) 23.0	66
K-Fe/MIL-88B	400	3.0	43.1	(C_2-C_{5+}) 36.7	67
MnO_2-K/Fe-Al-O	320	2.0	50	(C_{5+}) 43.0	68
ZrO_2-K/Fe-Al-O	320	2.0	30	(C_{5+}) 40.5	68
Fe-Zn-Zr @ Hbeta	340	5.0	16.8	(C_{5+}) 12.3	69
Cu-ZnO + HB zeolite	300	0.98	27.64	(C_2–C_{5+}) 45.5	70
In_2O_3 + HZSM-5	340	3.0	13.1	(C_{5+}) 80.0	71

The alkane selectivity was calculated based on all products except CO.

shown in Table 1 [48–71].

4.1.1 Fe-based catalysts for both RWGS reaction and Fischer-Tropsch reaction

Fe-based systems can catalyze both RWGS reaction and the hydrogenation of CO to alkanes [72,73]. The Fe_3O_4 and Fe_2O_3 phases of Fe catalysts can be reduced to Fe_5C_2, which is considered to be the active phase for the formation of long-chain alkanes [74].

4.1.1.1 Promoters

Bulk Fe catalyst in the absence of promoters presents some limitation in terms of stability, activity and selectivity to hydrocarbon products. Nevertheless, the addition of promoters such as alkali metals (Na, K, or Rb) [75,76] and transition metals (Mn, Cu, La, Zr, Cr, Mo, or Ta) [30,55,77] can remarkably enhance resistance to deactivation, and improve selectivity to long-chain alkanes. Alkali elements boost catalytic activity by acting as (i) an electronic promoter to shift product distributions to heavier hydrocarbons, (ii) a promotor of CO_2 adsorption through the introduction of basic sites, and (iii) an inhibitor of surface hydrogenation. Tuning the content of promoters may increase the olefin to paraffin ratio and the average molecular weight of the products [78]. Among the alkali promoters, K was reported to be the most effective one [79]. Besides those functions listed above, K may also increase the content of Fe_5C_2, and shifted Fe in the oxide and carbide phases to a more reduced state, thus increasing the relative exposure of active sites on the catalyst surface [80]. Recently, Na modified Fe-Zn catalysts were synthesized through a microwave-assisted hydrothermal method by using a Na-containing $ZnFe_2O_4$ precursor (Fig. 5a) [56]. Compared to bare Fe_2O_3, physically mixed ZnO-Fe_2O_3, and Na-free Fe-Zn catalysts, the $ZnFe_2O_4$-derived catalyst with a Na content of 0.08% (*w*) or beyond were superior, giving rise to a high CO_2 conversion, an improved C_{5+} liquid-fuel selectivity (~58%), and a high olefin to paraffin ratio (~11) in CO_2 hydrogenation (Fig. 5b).

Transition metals such as Mn can promote the reduction of Fe catalysts, and increase the dispersion of catalyst particles as well as the catalyst surface basicity. Relative to Mn, Zn presents a more basic surface, and enables higher CO and CO_2 adsorption. Zn also plays a role in stabilizing a catalyst, thereby limiting its initial deactivation, and granting better yields to alkanes than Mn [76]. The incorporation of other transition metals including Co, Ni, Cu, as well as noble metals such as Pd in Fe catalysts also enhanced the yield of C_{2+} alkanes from CO_2 hydrogenation [81].

Metal oxides can also serve as structural and electronic promoters [68]. It was reported that SiO_2, TiO_2, ZrO_2, HfO_2, CeO_2 and MnO_2 might modify the texture and surface reactivity of

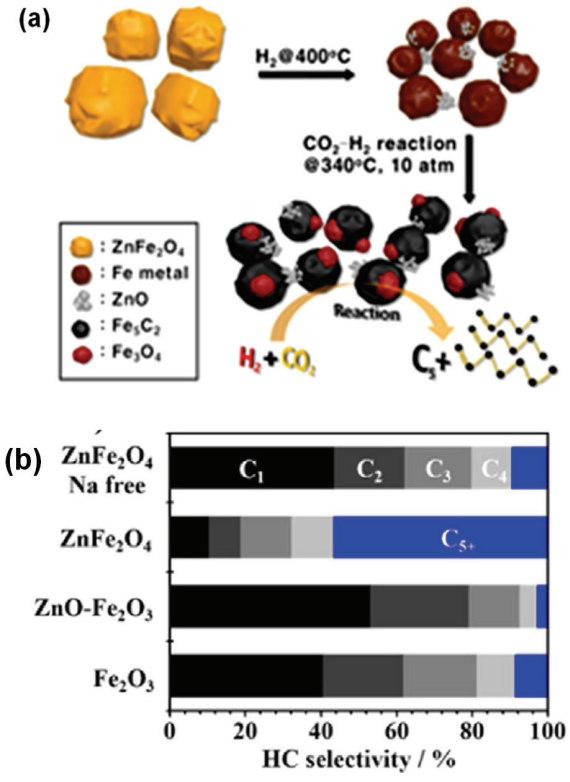

Fig. 5 (a) Structural evolution and mechanistic idea of $ZnFe_2O_4$-derived catalysts for CO_2 hydrogenation to yield C_{5+} liquid fuels. (b) CO-free hydrocarbon selectivity on Fe_2O_3, ZnO–Fe_2O_3, $ZnFe_2O_4$, and Na-free $ZnFe_2O_4$ catalysts [56].

K/Fe-Al-O catalyst, and therefore improved their performance in CO_2 hydrogenation (Fig. 6). The SiO_2 additive existed in the form of Fe-carbide, and selectively blocked the Fe-sites. While ZrO_2 existed in the form of grafted species (residual Fe-Al-O spinel), and oxide nanoparticles (NPs), which contributed to improved activities for both the RWGS reaction and the FT synthesis. This was attributed to the strong electronic interactions between ZrO_2 and neighboring metallic Fe-carbide phase.

4.1.1.2 Supports

Supports can offer high surface area, help to disperse the active components, and make the catalyst mechanically strong enough for long-time operation. A proper interaction between supports and the active sites can influence the whole process to a large extent [82].

Metal oxides, especially SiO_2, Al_2O_3, TiO_2, CeO_2 and ZrO_2, are the most commonly used supports for Fe-based catalysts [83,84,54]. Al_2O_3 exhibits abundant surface Al-OH groups, which favor the adsorption of CO intermediate. The large surface area of Al_2O_3 facilitated the formation of small iron carbide particles with high dispersion, affording C_{5+} hydrocarbons with selectivity of up to 31.1% [50]. It was found that only an appropriate pore size of Al_2O_3 falling in the range 7–10 nm could lead to optimum activities [57]. Oxygen defects on reduced and monoclinic ZrO_2 (*m*-ZrO_2) outperformed better than tetragonal ZrO_2 (*t*-ZrO_2) in adsorption and activation of CO_2 [85]. Murciano *et al*. [58] investigated the effect of the morphology of ceria supports on the catalytic properties of Fe-based catalysts. Among the three kinds of morphologies (particle, rod and cube), nanostructured ceria rods provided the highest hydrocarbon selectivity, while ceria cubes presented the highest olefin/paraffin ratio.

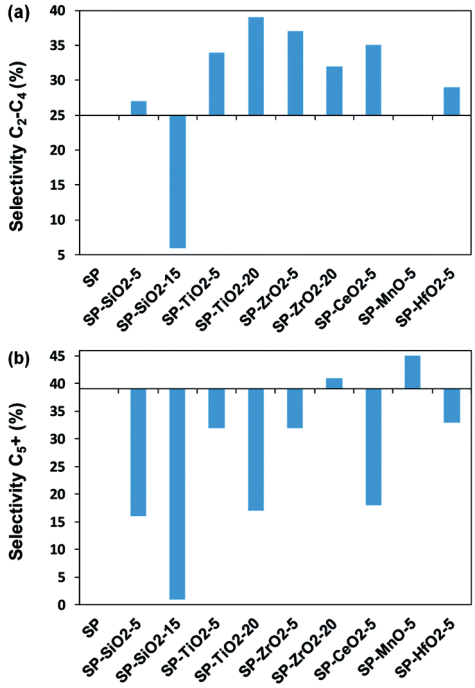

Fig. 6 Effects of additives on the catalytic performance of K/Fe–Al–O spinel in CO_2 hydrogenation: (a) selectivity to C_2–C_4 hydrocarbons, and (b) selectivity to C_{5+} hydrocarbons [68].

Some other supports, like carbon nanotubes (CNTs), Mo_2C, zeolite, MCM-41, and metal-organic frameworks (MOFs) have also been used in Fe catalysts [69,86]. CNTs have high specific surface area, multitudinous pore structure, superior chemical inertness, and eminent recycling characteristics. Fe NPs deposited on CNTs were reported to display low deactivation rates [87]. Surface modification of CNTs with nitrogen or oxygen is usually employed to provide strong anchoring sites for catalyst particles. Iron oxide NPs supported on N-doped CNTs were observed to be reduced more easily than those on O-doped CNTs [51,52]. Another interesting support is MOFs which have advantages such as large accessible surface areas, high porosity, and tunable functionalities. MOFs composed of abundant organic struts and regularly arranged metal nodes, can be transformed to carbon materials decorated with nano-structured metal species after annealing. As an example, porous carbon supported Fe NPs were synthesized *via* one-step pyrolysis of Fe-MIL-88B [67]. This catalyst displayed good selectivity to C_{5+} products (19.2%), and stability for CO_2 hydrogenation.

4.1.2 Co-based Fischer-Tropsch catalysts

Co catalysts are widely used in F-T synthesis particularly for the production of heavier hydrocarbons. It was suggested that Mn-modified Co_2C was the active phase to the formation of long-chain hydrocarbons [88]. While Co has very low RWGS reaction activity, and acts primarily as a methanation catalyst when CO_2 is used instead of CO [89]. To suppress methanation and improve catalytic performance of Co catalysts for CO_2 hydrogenation, the selection of promoters and supports is of importance.

4.1.2.1 Promoters

Note that unmodified cobalt systems tend to generate > 90% CH_4 in CO_2 hydrogenation [90,91]. To reduce the production of CH_4, small amounts of promoters including Li, Na, K, Mo, Cr and Mn were often added to Co-based catalysts [45,53,92]. For example, upon introduction of K to CoCu/TiO_2 catalyst, CH_4 formation was suppressed, and the main product was C_{5+}. But CO_2 conversion decreased, and CO selectivity increased [59]. Similarly, the addition of Mo and Na to Co enhanced the selectivity of C_{2+} alkanes [60].

4.1.2.2 Supports

Similar to Fe-based catalysts, the use of support (TiO_2, CeO_2, SiO_2, MgO and ZSM-5) affects the size of Co crystallites and their activity by providing a high surface area and metal-support interactions. For Co-Na-Mo catalysts, C_{5+} hydrocarbon selectivity was in the order of ZrO_2 < TiO_2 < Al_2O_3 < CeO_2 [60].

4.1.3 Bifunctional catalysts for both methanol synthesis and methanol-to-alkane transformation

Alkane products can also be obtained through cascade

catalysis combining methanol synthesis from CO_2 hydrogenation, and a subsequent MTH reaction [70,93]. Typical catalysts for the methanol synthesis from CO_2/H_2 include Cu-based materials (Cu supported on ZnO [94], Ga_2O_3 [95], ZrO_2 [96]) and noble metals (Pd [97], Pt [98], Au [99], Ag [100]), while the commonly used catalysts for the MTH process are zeolites [101].

A number of highly efficient bifunctional catalysts have been reported. Wang *et al*. [69] developed a Fe-Zn-Zr@zeolite core-shell catalyst, with Fe-Zn-Zr as the core and the zeolite (HZSM-5, Hbeta, and HY) as the shell. The Fe-Zn-Zr core promoted methanol synthesis, and also suppressed the unwanted RWGS reaction. While the zeolite shell provided a confined reaction space, and acidic sites to convert methanol into isoalkanes. The catalyst with a double-zeolite (HZSM-5 and Hbeta) shell exhibited even higher performance for isoalkane synthesis, resulting from a synergistic effect between the two zeolites. A bifunctional catalyst comprising In_2O_3 and HZSM-5 was reported, which enabled selective production of liquid fuels with C_{5+} fractions as high as 78.6% from CO_2 hydrogenation (Fig. 7) [71]. The oxygen vacancies on the In_2O_3 surface benefited CO_2 activation and hydrogenation. The undesirable RWGS reaction was inhibited by moving the two components into a closer proximity (from Fig. 7b to Fig. 7d), yielding a high selectivity for hydrocarbons.

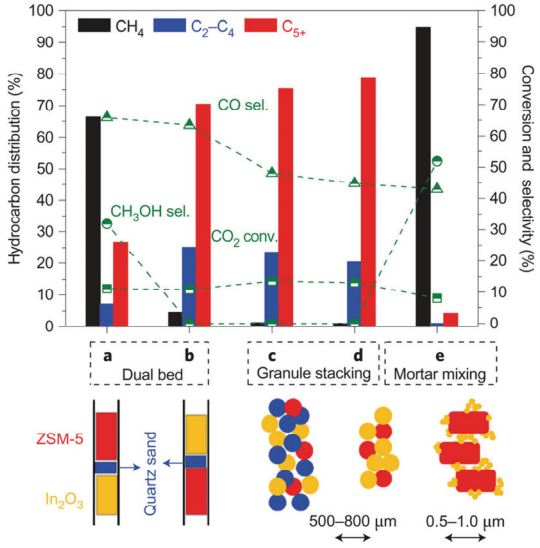

Fig. 7 Influence of the integration manner of the active components on catalytic behaviours under the same conditions. (a) Dual-bed configuration with In_2O_3 packed below HZSM-5 and separated by a layer of quartz sand. (b) HZSM-5 packed below In_2O_3 and separated by quartz sand. (c) Stacking of granules with the In_2O_3, HZSM-5 and quartz sand particle sizes of 250–380 μm. (d) In_2O_3 and HZSM-5 particles well mixed without quartz sand. (e) In_2O_3 and HZSM-5 mixed with an agate mortar [71].

4.2 C_{2+} olefins

Synthesis of lower olefins from CO_2 hydrogenation has achieved advances in recent years [102,103]. Relevant solid catalysts are summarized in Table 2 [41,103–116]. The formation of short-chain olefins is always accompanied with CH_4 and > C_4 hydrocarbons [117]. Despite that a high selectivity of C_2–C_4 olefins up to 65.2% has been obtained at low CO_2 conversion (25.7%), further improvement is still needed to control the chain growth.

4.2.1 Catalysts for both RWGS reaction and CO hydrogenation

As the case of alkane production, light olefins can be produced from CO_2 through a combined route of RWGS reaction and subsequent CO hydrogenation. A catalyst needs to be active for both RWGS reaction and CO hydrogenation under the same operating conditions. Fe-based catalysts are predominantly used for the synthesis of C_2–C_4 olefins [104,63,118].

4.2.1.1 Promoters

Fe catalysts alone show insufficient selectivities to olefins. This can be addressed by adding promoters [119]. The promoters

Table 2 Reported catalytic systems for the synthesis of light olefins (C_2–C_4) by CO_2 hydrogenation.

Catalysts	Temperature/ºC	Pressure/MPa	CO_2 conversion/%	Olefin selectivity/%	Ref.
K-Fe/ZrO_2	340	2.0	43	30.2	103
B-K/Fe oxide	340	2.0	38	31.6	104
Na/Fe_3O_4	320	3.0	40.5	38.8	105
Fe-In/SiO_2	370	0.1	25.7	65.2	106
Fe-Cu-K_2O-La_2O_3/ZrO_2-SiO_2	340	0.1	51.4	26.6	107
K-Fe-Zr	320	2.0	54.36	53.6	108
Fe/ZSM-5	350	0.1	83.03	14.1	109
ZIF-8/Fe_2O_3	300	3.0	21	20.0	110
In_2O_3/ZrO_2 + SAPO-34	400	1.5	20	85.5	111
K-Zn/Fe_2O_3	300	0.5	51.03	45.6	112
K/Fe_3O_4	300	0.5	45	36.0	113
K/Fe-Al-O	320	2.0		24.0	114
Fe-Co-K/Al_2O_3	320	2.0	49	47.0	115
K-Fe-Co/Al_2O_3	300	1.0	31	22.6	116
ZnZrO/SAPO	380	2.0	12.6	80.1	41

The olefin selectivity was calculated based on all products except CO.

can enhance structural and chemical properties, and stabilize active components [120]. In addition, these promoters were supposed to increase CO adsorption while decrease hydrogen adsorption on the catalytic surface, thereby increasing the surface coverage of dissociatively adsorbed CO. A high CO coverage can inhibit the olefin readsorption rate, leading to higher olefin selectivity [105]. Alternatively, a strong interaction between an active phase (such as Fe_2O_3) and a support (such as K_2O), may favorably suppress the hydrogenation of olefins [113].

The addition of alkali metals (Li, Na, K, Rb and Cs) to Fe-based catalysts could improve the selectivity of C_2–C_4 olefins. The yield of C_2–C_4 olefins increased in the following order: Fe < Li^+-modified Fe < Na^+-modified Fe < Cs^+-modified Fe < K^+-modified Fe < Rb^+-modified Fe [121,103]. Cheng *et al.* [122] investigated the effect of Na on the structure and catalytic performance of supported Fe catalysts. Olefin selectivity increased with the amount of Na, while alkane selectivity decreased inversely. It seems that Na can promote the surface basicity of catalyst, which favors for olefin production.

In addition to alkali metals, group 11 metals (Cu, Ag, and Au) and group 13 metals (Al, Ga, and In) can also act as promoters [106]. Among the Group 11 metals tested, Au in Fe/SiO_2 catalyst performed the highest selectivity of C_2–C_4. However, In was far more effective than the others, affording a C_2–C_4 olefin selectivity of 65.2% upon the addition of 3% (mass fraction) In to the system. Theoretical investigations suggested that In_2O_3 promoted CO_2 activation and hydrogen adsorption through a dissociative process [123]. Meanwhile, In_2O_3 was also active for the dehydrogenation of propane by utilising CO_2 as a mild oxidant, and high levels of C_2–C_4 olefins were attained [124].

Ce, La and Mn have also been used to modify Fe catalysts [107]. Mn may function as both structural and electronic promoters, imparting improved activity and selectivity toward light olefins [55,125,126]. The addition of CeO_2 in Fe/Mn/K catalyst resulted in an approximately 22% increase in CO_2 conversion, and a 5% increase in olefin formation [127]. It was speculated that CeO_2 accommodated large amounts of hydrogen within its lattice. Smaller CeO_2 particles had more lattice defects/oxygen vacancies, thus being more easily reduced than those larger ones. Tuning the particle size of CeO_2 allowed one to tailor the catalyst's activity and selectivity.

Other reported metals to promote CO_2 conversion include Cr and Zn [128,129]. Zn likely increased catalyst surface basicity, enhancing selectivity for C_2–C_4 olefins [130].

4.2.1.2 Supports

The widely used catalyst supports include SiO_2, Al_2O_3, TiO_2, ZrO_2, mesoporous carbon, and CNTs. Among these supports, ZrO_2 supported K-Fe catalyst provided the highest selectivity (42.3%) and yield (13%) to lower olefins. Two aspects may be relevant. On the one hand, ZrO_2 offered adsorption sites for surface reaction intermediates. On the other hand, the synergistic effect of K and ZrO_2 hindered the re-adsorption of olefins, improving CO_2 hydrogenation activity towards light olefins [103]. Graphitic carbon can enhance electron abundance on those metal-rich sites, resulting in high activity. The inner concave surface of graphitic carbon both Fe_3O_4@carbon core-shell nanostructures and Fe NPs encapsulated inside the lumen of CNTs, was calculated to be able to improve the reducibility of iron oxides relative to the outer convex surface [131]. Graphitic carbon shells exhibit lower energy barriers for the surface migration of hydrogen as compared with other supports like Al_2O_3 or SiO_2, which in turn leads to lower selectivity of olefin [51]. Fe, Fe_5C_2 and Fe_3O_4 encased in partially graphitized carbon shells were synthesized by Gupta and co-workers and examined for CO_2 hydrogenation (Fig. 8a). The olefin/paraffin ratio (O/P) was found to increase when the carbon content was increased from 0.5 to 1.5. However, further increasing the carbon content by deposition of excess carbon around the Fe_3O_4 core probably hindered the accessibility of reactants to the Fe active sites, and reduced the O/P (Fig. 8b) [108].

ZSM-5 zeolite with suitable acidity and pore size can also act as a support for Fe catalysts to improve the selectivity of light olefins [109]. MOFs, such as ZIF-8 can be stable up 300 ºC, making such porous materials a potential support for high temperature and high pressure catalytic reactions. ZIF-8 compares more favorably than MIL-53(Al) and γ-Al_2O_3 supports in terms of CO_2 conversion and olefin selectivity [110]. Larger ZIF-8 crystals corresponded to lower olefin selectivity

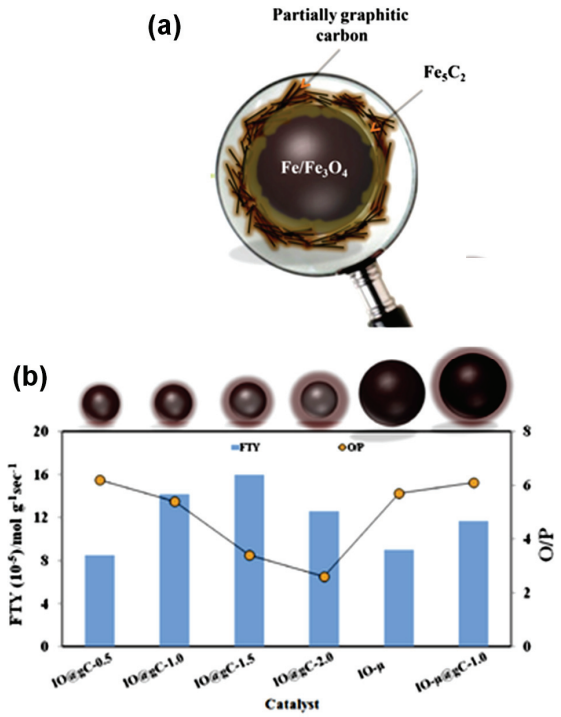

Fig. 8 (a) A cartoon of Fe_3O_4@carbon core-shell nanostructure. (b) Fe time yield (FTY) and O/P ratio of catalysts with different carbon contents in CO_2 hydrogenation [108].

due to occurrence of secondary reaction of hydrogenation during the internal diffusion process.

4.2.2 Bifunctional catalysts for both methanol synthesis and methanol-to-olefin transformation

Hybrid catalysts that are active for both methanol synthesis and MTH conversion have been also used for the production of olefins. Zeolites with weak acidic sites and narrow micropores may facilitate the selective formation of light olefins. SAPO is such kind of zeolite [132], which could yield C_2–C_4 olefins with selectivities of up to 80% [111]. Indeed, a ZnZrO/SAPO catalyst (Fig. 9a,b) gave 80% selectivity of C_2–C_4 olefins, 14% C_2–C_4 alkanes, 3% CH_4, and 3% C_{5+} among all hydrocarbon products at a CO_2 conversion of 12.6% (Fig. 9c) [41]. CO_2 conversion increased with increasing reaction temperatures, but the olefin selectivity decreased. This is due to the fact that higher temperatures favor RWGS reaction. To attain a high yield of lower olefins, the reaction conditions were optimized with reaction temperature of 380 °C, space velocity of 3600 $mL·g^{-1}·h^{-1}$.

4.3 High alcohols

High alcohols ($C_{2+}OH$), relative to CH_3OH are more desirable products as neat fuels, fuel additives, and hydrogen resources in fuel cells [133,134]. Recent years have seen great advances in the synthesis of high alcohols with CO_2 by homogeneous catalysis [135−138]. In the following part, we focus on significant achievements that have been made on heterogeneous catalysis of CO_2 hydrogenation towards high alcohols. Recent advances in this regard are summarized in Table 3 [43,76,139-148].

Noble metals (Rh, Pt, Ru) and transition metals (Cu, Fe, Co) on metal oxide supports (e.g., Fe_2O_3, Co_3O_4, ZrO_2, Al_2O_3, SiO_2) have been widely used for CO_2 hydrogenation to synthesize high alcohols [134]. As opposed to single metals, bimetallic catalysts (such as CuFe, CuZn) can create a synergism between the two metals, leading to higher catalytic efficiency [139,140,76]. A MoCoK sulfide catalyst showed a potential for C_{2+} alcohol production with C_{2+} alcohol selectivity of 10.9% from CO_2 hydrogenation. In this hybrid catalyst, Co

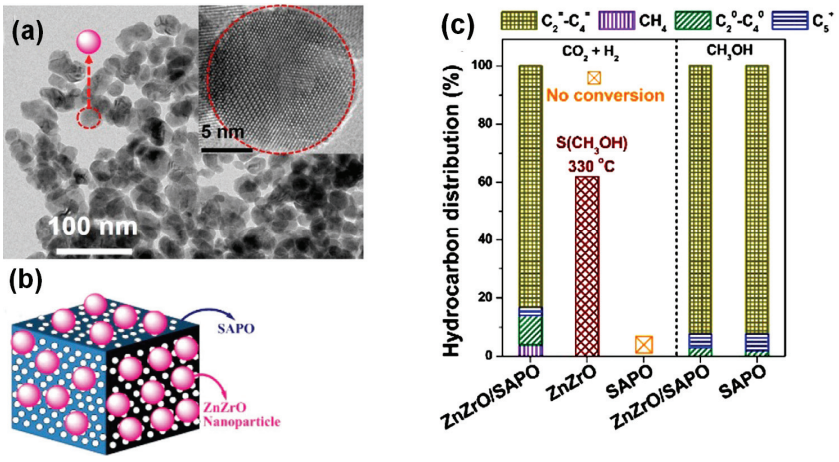

Fig. 9 (a) TEM and HRTEM (inset) images of ZnZrO. (b) Schematic description of ZnZrO/SAPO. (c) Catalytic results of CO_2 hydrogenation on ZnZrO/SAPO, ZnZrO and SAPO, and methanol conversion on ZnZrO/SAPO and SAPO [41].

Table 3 Reported catalysts for the synthesis of high alcohols by CO_2 hydrogenation.

Catalysts	Temperature/°C	Pressure/MPa	CO_2 conversion/%	$C_{2+}OH$ selectivity/%	Ref.
Li-Rh/SiO_2	240	5.0	7.0	Ethanol 15.5	43
K-Cu/$ZnFeO_4$	300	6.0	42.3	(C_2–C_5)~32.0 (*w*)	76
K_2O-Cu-Zn-Fe/ZrO_2	320	3.0	25.49	(C_2–C_4) 8.9	139
K/Cu-Zn	350	6.0	19.97	Ethanol 7.6	140
Mn-Co-K/AC	320	5.0	28.8	C_{2+} 10.9	141
Pt/Co_3O_4	340	2.0	25.5	(C_{2+}) 22.7	142
Fe-Cu/MCM-41	350	1.0	3	Ethanol 99.0	143
K-Cu/ZnO	350	6.0	27.18	Ethanol 7.6	144
Co-Na/SiO_2	220	2.1	7.6	Ethanol 7.9	145
Rh-Co/SiO_2	260	5.0	25.2	Ethanol 1.2	146
Ir-Mo/SiO_2	200	4.9	11.9	(C_2–C_3) 6.3	147
Cu-Zn-Al-K-Ga-Pd+ Fe-Cu-Al-K	330	8.0	47	Ethanol 17.4	148

The alcohol selectivity was calculated based on all products except CO.

served as an electron-donating additive, and shifted the binding energy of Mo 3d to a lower value. Such shift was related to the interaction between Mo and Co. It was found that the interaction between Co and Mo was enhanced when using activated carbon as a support, whereas the interaction became weakened in the case of SiO_2, Al_2O_3, and TiO_2 [141].

In addition to composition, the structure of catalyst supports also influences catalytic activity and product selectivity. Ouyang *et al*. [142] synthesized two different morphologies of Co_3O_4 (nanorods and nanoplates) and used them to support Pt NPs for CO_2 hydrogenation. The nanoplates were found to be reduced more easily than the nanorods, forming some metallic Co. The metallic Co had strong hydrogenation ability, and produced CH_4 dominantly. Whereas the Co_3O_4 nanorods were reduced to CoO, which had a large mobility of surface oxygen. The surface oxygen was easily reduced to generate oxygen vacancies. The synergic effect of Pt and Co, and oxygen vacancies of reduced Co_3O_4 facilitated the production of high alcohols with C_{2+} alcohol selectivity of 22.7%. Bimodal MCM-41 (T) was revealed to be a better support for FeCu catalysts towards CO_2 hydrogenation than unimodal MCM-41 (SS), yielding higher CO_2 conversion (1.2–2.1 times). The MCM-41 (T) catalyst loaded with 3% (*w*) Fe and 10% (*w*) Cu exhibited an alcohol (methanol and ethanol) selectivity of 80%–99% at low reaction temperature (160–200 °C). Such high activity was correlated with the pore characteristics of the support. The existence of larger mesopores in bimodal MCM-41 (T) was speculated to promote the formation of bigger metal particles, resulting in weaker metal-support interactions, beneficial to this reaction and yield of alcohols [143].

5 Summary and outlook

Mitigating the effects caused by waste CO_2 emissions continues to be a critical issue to modern society. The hydrogenation of CO_2 by using renewable hydrogen offers an attractive approach for conversion of CO_2 into fuels or value-added chemicals. High (C_{2+}) hydrocarbons and oxygenates are desirable hydrogenation products that bear advantages of high energy densities and compatibility with end-use infrastructures. However, the hydrogenation of CO_2 to yield C_{2+} products remains an ongoing challenge due to high C—C coupling barriers.

CO_2 can be hydrogenated to hydrocarbons *via* CO intermediate or CH_3OH intermediate. The former involves an integration of RWGS reaction and FT-like synthesis. While the latter couples CH_3OH synthesis with MTH process. The design of catalyst is the key to accomplishing the selective yield of C_{2+} fuels. Advanced catalysts need to be active for both reductive step and C—C coupling step. ZnZrO/SAPO and In_2O_3/ZrO_2/SAPO tandem catalysts gave the highest selectivity for lower olefins (80%–90%) *via* CH_3OH intermediate to date. Fe or Co-based catalysts have been widely used to catalyze the hydrogenation of CO_2 to C_{2+} hydrocarbons *via* CO intermediate. The incorporation of alkali metals and transition metals in Fe-based catalysts can enhance catalyst resistance to deactivation as well as CO_2 conversion to hydrocarbons. K appears to be the most effective alkali metal promoters, especially for the production of olefins. For Co-based catalysts, promoters play a role in suppressing methanation rate and improve selectivities to liquid hydrocarbons (C_{5+}). FeC_x (possibly Hägg iron carbide, X-Fe_5C_2) in Fe-based catalysts is considered to be the major active site for the synthesis of liquid hydrocarbons from CO_2. Likewise, Co_2C stabilized with a promoter (Mn) may be the active centers in FT synthesis [88], although unpromoted Co_2C is unstable in reaction conditions and is readily reduced to Co^0. In addition to FeC_x, Co_2C, and Mo_2C that have shown promising activities in FT synthesis, other metal or bimetal carbide catalysts deserve future exploration, which may give interesting catalytic properties for CO_2 conversion to C_{2+} species.

High alcohols (mostly ethanol) have been produced by using a hybrid tandem catalyst. CO_2 activation occurs on Cu-based catalysts, noble metals or metal oxides with oxygen vacancies, whilst C—C coupling takes place within the pores of zeolites. The activation mechanism, C—C precise coupling, and synergy control between the two active components require further research.

In spite of these encouraging results, both the time-yields and selectivities of C_{2+} products achieved so far are unsatisfactory. No commercial implementation has yet reached. In addition, the nature of active sites, and interactions among active phase, promoter, and support are still under debate. Developing *in situ* (spectroscopic) characterization techniques will help build more precise theoretical models to gain deeper insights into catalytic reaction pathways and structure-activity relationships. The combination of calculations and experiments will further aid catalyst design to increase the number of active sites and intrinsic activity of each active site. This also facilitates the development of novel robust catalysts with cooperative functionalities to achieve both high CO_2 conversion and C_{2+} product selectivity.

References

(1) Kondratenko, E. V.; Mul, G.; Baltrusaitis, J.; Larrazábal, G. O.; Pérez, R. J. *Energ. Environ. Sci.* **2013,** *6*, 3112. doi: 10.1039/c3ee41272e

(2) Caldeira, K.; Wickett, M. E. *Nature* **2003,** *425*, 365. doi: 10.1038/425365a

(3) Porosoff, M. D.; Yan, B. H.; Chen, J. G. G. *Energ. Environ. Sci.* **2016,** *9*, 62. doi: 10.1039/c5ee02657a

(4) Centi, G.; Quadrelli, E. A.; Perathoner, S. *Energ. Environ. Sci.* **2013,** *6*, 1711. doi: 10.1039/c3ee00056g

(5) Ma, T.; Fan, Q.; Tao, H. C.; Han, Z. S.; Jia, M. W.; Gao, Y. N.; Ma, W. J.; Sun, Z. Y. *Nanotechnology* **2017,** *28*, 472001.

doi: 10.1088/1361-6528/Aa8f6f

(6) Sun, Z. Y.; Talreja, N.; Tao, H. C.; Texter, J.; Strunk, J.; Muhler, M.; Chen, J. F. *Angew. Chem. Int. Ed.* **2018**, doi: 10.1002/ange.201710509

(7) Sun, Z. Y.; Ma, T.; Tao, H. C.; Fan, Q.; Han, B. X. *Chem* **2017,** *3*, 560. doi: 10.1016/j.chempr.2017.09.009

(8) Zhang, L.; Zhao, Z. J.; Gong, J. L. *Angew. Chem. Int. Ed.* **2017,** *56*, 11326. doi: 10.1002/anie.201612214

(9) Tao, H. C.; Sun, X. F.; B., S.; Han, Z. S.; Zhu, Q. G.; R., A. W.; Ma, T.; Fan, Q.; X., H. B.; Jung, Y.; Sun, Z. Y. *Chem. Sci.* **2018,** *9*, 483. doi: 10.1039/C7SC03018E

(10) Tao, H. C.; Gao, Y. A.; Talreja, N.; Guo, F.; Texter, J.; Yan, C.; Sun, Z. Y. *J. Mater. Chem. A* **2017,** *5*, 7257. doi: 10.1039/c7ta00075h

(11) Habisreutinger, S. N.; Schmidt-Mende, L.; Stolarczyk, J. K. *Angew. Chem. Int. Ed.* **2013,** *52*, 7372. doi: 10.1002/anie.201207199

(12) Chang, X. X.; Wang, T.; Gong, J. L. *Energ. Environ. Sci.* **2016,** *9*, 2177. doi: 10.1039/c6ee00383d

(13) Behrens, M.; Studt, F.; Kasatkin, I.; Kuhl, S.; Havecker, M.; Abild-Pedersen, F.; Zander, S.; Girgsdies, F.; Kurr, P.; Kniep, B. L.; *et al. Science* **2012,** *336*, 893. doi: 10.1126/science.1219831

(14) Song, Q. W.; Zhou, Z. H.; He, L. N. *Green Chem.* **2017,** *19*, 3707. doi: 10.1039/c7gc00199a

(15) Saeidi, S.; Najari, S.; Fazlollahi, F.; Nikoo, M. K.; Sefidkon, F.; Klemes, J. J.; Baxter, L. L. *Renew. Sust. Energ. Rev.* **2017,** *80*, 1292. doi: 10.1016/j.rser.2017.05.204

(16) Dai, W. L.; Luo, S. L.; Yin, S. F.; Au, C. T. *Appl. Catal. A-Gen.* **2009,** *366*, 2. doi: 10.1016/j.apcata.2009.06.045

(17) Centi, G.; Perathoner, S. *Catal. Today* **2009,** *148*, 191. doi: 10.1016/j.cattod.2009.07.075

(18) Galvis, H. M. T.; Bitter, J. H.; Khare, C. B.; Ruitenbeek, M.; Dugulan, A. I.; de Jong, K. P. *Science* **2012,** *335*, 835. doi: 10.1126/science.1215614

(19) Ayodele, O. B. *J. CO_2 Util.* **2017,** *20*, 368. doi: 10.1016/j.jcou.2017.06.015

(20) Prieto, G. *ChemSusChem* **2017,** *10*, 1056. doi: 10.1002/cssc.201601591

(21) Chianelli, R. R.; Lyons, J. E.; Mills, G. A. *Catal. Today* **1994,** *22*, 361. doi: 10.1016/0920-5861(94)80110-X

(22) Yang, H. Y.; Zhang, C.; Gao, P.; Wang, H.; Li, X. P.; Zhong, L. S.; Wei, W.; Sun, Y. H. *Catal. Sci. Technol.* **2017,** *7*, 4580. doi: 10.1039/c7cy01403a

(23) Yan, X. C.; Guo, H.; Yang, D. J.; Qiu, S. L.; Yao, X. D. *Curr. Org. Chem.* **2014,** *18*, 1335. doi: 10.2174/1385272819666140424212948

(24) Centi, G.; Iaquaniello, G.; Perathoner, S. *ChemSusChem* **2011,** *4*, 1265. doi: 10.1002/cssc.201100313

(25) Alvarez, A.; Bansode, A.; Urakawa, A.; Bavykina, A. V.; Wezendonk, T. A.; Makkee, M.; Gascon, J.; Kapteijn, F. *Chem. Rev.* **2017,** *117*, 9804. doi: 10.1021/acs.chemrev.6b00816

(26) Goeppert, A.; Czaun, M.; Jones, J. P.; Prakash, G. K. S.; Olah, G. A. *Chem. Soc. Rev.* **2014,** *43*, 7995. doi: 10.1039/c4cs00122b

(27) Wang, W.; Wang, S.; Ma, X.; Gong, J. *Chem. Soc. Rev.* **2011,** *40*, 3703. doi: 10.1039/c1cs15008a

(28) Pour, A. N.; Karimi, J.; Housaindokht, M.; Hashemian, M. *React. Kinet. Mech. Cat.* **2017,** *122*, 605. doi: 10.1007/s11144-017-1242-7

(29) Riedel, T.; Schaub, G.; Jun, K. W.; Lee, K. W. *Ind. Eng. Chem. Res.* **2001,** *40*, 1355. doi: 10.1021/Ie000084k

(30) Rodemerck, U.; Holena, M.; Wagner, E.; Smejkal, Q.; Barkschat, A.; Baerns, M. *ChemCatChem* **2013,** *5*, 1948. doi: 10.1002/cctc.201200879

(31) Torrente-Murciano, L.; Mattia, D.; Jones, M. D.; Plucinski, P. K. *J. CO_2 Util.* **2014,** *6*, 34. doi: 10.1016/j.jcou.2014.03.002

(32) Liang, B. L.; Duan, H. M.; Hou, B. L.; Su, X.; Huang, Y. Q.; Wang, A. Q.; Wang, X. D.; Zhang, T. *Chem. Ind. Eng. Prog.* **2015,** *34*, 3746. doi: 10.16085/j.issn.1000-6613.2015.10.035

(33) Kim, S. S.; Lee, H. H.; Hong, S. C. *Appl. Catal. A-Gen.* **2012,** *423*, 100. doi: 10.1016/j.apcata.2012.02.021

(34) Wang, L. C.; Khazaneh, M. T.; Widmann, D.; Behm, R. J. *J. Catal.* **2013,** *302*, 20. doi: 10.1016/j.jcat.2013.02.021

(35) Brady, R. C.; Pettit, R. *J. Am. Chem. Soc.* **1981,** *103*, 1287. doi: 10.1002/chin.198125169

(36) Gunasooriya, G. T. K. K.; van Bavel, A. P.; Kuipers, H. P. C. E.; Saeys, M. *ACS Catal.* **2016,** *6*, 3660. doi: 10.1021/acscatal.6b00634

(37) Ojeda, M.; Nabar, R.; Nilekar, A. U.; Ishikawa, A.; Mavrikakis, M.; Iglesia, E. *J. Catal.* **2010,** *272*, 287. doi: 10.1016/j.jcat.2010.04.012

(38) Schweicher, J.; Bundhoo, A.; Kruse, N. *J. Am. Chem. Soc.* **2012,** *134*, 16135. doi: 10.1021/ja3068484

(39) Chakrabarti, D.; Gnanamani, M. K.; Shafer, W. D.; Ribeiro, M. C.; Sparks, D. E.; Prasad, V.; de Klerk, A.; Davis, B. H. *Ind. Eng. Chem. Res.* **2015,** *54*, 6438. doi: 10.1021/acs.iecr.5b01402

(40) Flory, P. J. *J. Am. Chem. Soc.* **1936,** *58*, 1877. doi: 10.1021/ja01301a016

(41) Li, Z. L.; Wang, J. J.; Qu, Y. Z.; Liu, H. L.; Tang, C. Z.; Miao, S.; Feng, Z. C.; An, H. Y.; Li, C. *ACS Catal.* **2017,** *7*, 8544. doi: 10.1021/acscatal.7b03251

(42) Chang, C. D.; Silvestri, A. J. *J. Catal.* **1977,** *47*, 249. doi: 10.1016/0021-9517(77)90172-5

(43) Kusama, H.; Okabe, K.; Sayama, K.; Arakawa, H. *Catal. Today* **1996,** *28*, 261. doi: 10.1016/0920-5861(95)00246-4

(44) Yang, Y. Z.; Lin, T. J.; Qi, X. Z.; Yu, F.; An, Y. L.; Li, Z. J.; Dai, Y. Y.; Zhong, L. S.; Wang, H.; Sun, Y. H. *Appl. Catal. A-Gen.* **2018,** *549*, 179. doi: 10.1016/j.apcata.2017.09.037

(45) Gnanamani, M. K.; Jacobs, G.; Keogh, R. A.; Shafer, W. D.; Sparks, D. E.; Hopps, S. D.; Thomas, G. A.; Davis, B. H. *Appl. Catal. A-Gen.* **2015,** *499*, 39. doi: 10.1016/j.apcata.2015.03.046

(46) Kangvansura, P.; Chew, L. M.; Saengsui, W.; Santawaja, P.; Poo-arporn, Y.; Muhler, M.; Schulz, H.; Worayingyong, A. *Catal. Today* **2016,** *275*, 59. doi: 10.1016/j.cattod.2016.02.045

(47) Kurakata, H.; Izumi, Y.; Aika, K. *Chem. Commun.* **1996,** *3*, 389. doi: 10.1039/Cc9960000389

(48) Dorner, R. W.; Hardy, D. R.; Williams, F. W.; Willauer, H. D. *Catal. Commun.* **2010,** *11*, 816. doi: 10.1016/j.catcom.2010.02.024

(49) Satthawong, R.; Koizumi, N.; Song, C. S.; Prasassarakich, P. *J. CO_2 Util.* **2013,** *3–4*, 102. doi: 10.1016/j.jcou.2013.10.002

(50) Ding, F. S.; Zhang, A. F.; Liu, M.; Zuo, Y.; Li, K. Y.; Guo, X. W.; Song, C. S. *Ind. Eng. Chem. Res.* **2014,** *53*, 17563. doi: 10.1021/ie5031166

(51) Chew, L. M.; Ruland, H.; Schulte, H. J.; Xia, W.; Muhler, M. *J. Chem. Sci.* **2014,** *126*, 481. doi: 10.1007/s12039-014-0591-2

(52) Chew, L. M.; Kangvansura, P.; Ruland, H.; Schulte, H. J.; Somsen, C.; Xia, W.; Eggeler, G.; Worayingyong, A.; Muhler, M. *Appl. Catal. A-Gen.* **2014,** *482*, 163. doi: 10.1016/j.apcata.2014.05.037

(53) Owen, R. E.; O'Byrne, J. P.; Mattia, D.; Plucinski, P.; Pascu, S. I.; Jones, M. D. *Chem. Commun.* **2013,** *49*, 11683. doi: 10.1039/c3cc46791k

(54) Ding, F. S.; Zhang, A. F.; Liu, M.; Guo, X. W.; Song, C. S. *RSC Adv.* **2014,** *4*, 8930. doi: 10.1039/c3ra44485f

(55) Al-Dossary, M.; Ismail, A. A.; Fierro, J. L. G.; Bouzid, H.; Al-Sayari, S. A. *Appl. Catal. B-Environ.* **2015,** *165*, 651. doi: http://dx.doi.org/10.1016/j.apcatb.2014.10.064

(56) Choi, Y. H.; Eun, C. R.; Eun, H. K.; Kwang, Y. K.; Youn, J. J.; Kyeong, N. K.; Sun, H. C.; Jang, J. H.; Jae, S. L. *ChemSusChem* **2017,** *10*, 1. doi: 10.1002/cssc.201701437

(57) Xie, T. Z.; Wang, J. Y.; Ding, F. S.; Zhang, A. F.; Li, W. H.; Guo, X. W.; Song, C. S. *J. CO_2 Util.* **2017,** *19*, 202. doi: 10.1016/j.jcou.2017.03.022

(58) Torrente, M. L.; Chapman, R. S. L.; Narvaez-Dinamarca, A.; Mattia, D.; Jones, M. D. *Phys. Chem. Chem. Phys.* **2016,** *18*, 15496. doi: 10.1039/c5cp07788e

(59) Shi, Z. B.; Yang, H. Y.; Gao, P.; Li, X. P.; Zhong, L. S.; Wang, H.; Liu, H. J.; Wei, W.; Sun, Y. H. *Catal. Today* **2017,** doi: 10.1016/j.cattod.2017.09.053

(60) Owen, R. E.; Plucinski, P.; Mattia, D.; Torrente-Murciano, L.; Ting, V. P.; Jones, M. D. *J. CO_2 Util.* **2016,** *16*, 97. doi: 10.1016/j.jcou.2016.06.009

(61) Rafati, M.; Wang, L. J.; Shahbazi, A. *J. CO_2 Util.* **2015,** *12*, 34. doi: 10.1016/j.jcou.2015.10.002

(62) Xu, W. Q.; Ramirez, P. J.; Stacchiola, D.; Brito, J. L.; Rodriguez, J. A. *Catal. Lett.* **2015,** *145*, 1365. doi: 10.1007/s10562-015-1540-5

(63) Albrecht, M.; Rodemerck, U.; Schneider, M.; Broring, M.; Baabe, D.; Kondratenko, E. V. *Appl. Catal. B-Environ.* **2017,** *204*, 119. doi: 10.1016/j.apcatb.2016.11.017

(64) Choi, Y. H.; Jang, Y. J.; Park, H.; Kim, W. Y.; Lee, Y. H.; Choi, S. H.; Lee, J. S. *Appl. Catal. B-Environ.* **2017,** *202*, 605. doi: 10.1016/j.apcatb.2016.09.072

(65) Riedel, T.; Schaub, G.; Jun, K. W.; Lee, K. W. *Ind. Eng. Chem. Res.* **2001,** *40*, 1355. doi: 10.1021/Ie000084k

(66) Li, W. H.; Zhang, A.; Jiang, X.; Janik, M. J.; Qiu, J.; Liu, Z. M.; Guo, X. W.; Song, C. S. *J. CO_2 Util.* **2017,** *23,* 219. doi: 10.1016/j.jcou.2017.07.005

(67) Liu, J.; Zhang, A.; Liu, M.; Hu, S.; Ding, F.; Song, C.; Guo, X. *J. CO_2 Util.* **2017,** *21*, 100. doi: 10.1016/j.jcou.2017.06.011

(68) Samanta, A.; Landau, M. V.; Vidruk-Nehemya, R.; Herskowitz, M. *Catal. Sci. Technol.* **2017,** *7*, 4048. doi: 10.1039/c7cy01118k

(69) Wang, X. X.; Yang, G. H.; Zhang, J. F.; Chen, S. Y.; Wu, Y. Q.; Zhang, Q. D.; Wang, J. W.; Han, Y. Z.; Tan, Y. S. *Chem. Commun.* **2016,** *52*, 7352. doi: 10.1039/c6cc01965j

(70) Fujiwara, M.; Sakurai, H.; Shiokawa, K.; Iizuka, Y. *Catal. Today* **2015,** *242*, 255. doi: 10.1016/j.cattod.2014.04.032

(71) Gao, P.; Li, S. G.; Bu, X. N.; Dang, S. S.; Liu, Z. Y.; Wang, H.; Zhong, L. S.; Qiu, M. H.; Yang, C. G.; Cai, J.; Wei, W.; Sun, Y. H. *Nat. Chem.* **2017,** *9*, 1019. doi: 10.1038/Nchem.2794

(72) Mark, E. D.; Burtron, H. D. *Appl. Catal. A-Gen.* **1996,** *138*, 319. doi: 10.1016/0926-860X(95)00306-1

(73) Landau, M. V.; Meiri, N.; Utsis, N.; Nehemya, R. V.; Herskowitz, M. *Ind. Eng. Chem. Res.* **2017,** *56*, 13335. doi: 10.1021/acs.iecr.7b01817

(74) Gnanamani, M. K.; Jacobs, G.; Hamdeh, H. H.; Shafer, W. D.; Davis, B. H. *Catal. Today* **2013,** *207*, 50. doi: 10.1016/j.cattod.2012.02.059

(75) Kishan, G.; Lee, M. W.; Nam, S. S.; Choi, M. J.; Lee, K. W. *Catal. Lett.* **1998,** *56*, 215. doi: 10.1023/A:1019089919614

(76) Li, S. G.; Guo, H. J.; Luo, C. R.; Zhang, H. R.; Xiong, L.; Chen, X. D.; Ma, L. L. *Catal. Lett.* **2013,** *143*, 345. doi: 10.1007/s10562-013-0977-7

(77) Yan, S. R.; Jun, K. W.; Hong, J. S.; Choi, M. J.; Lee, K. W. *Appl.*

Catal. A-Gen. **2000,** *194*, 63. doi: 10.1016/S0926-860X(99)00354-3

(78) Visconti, C. G.; Martinelli, M.; Falbo, L.; Fratalocchi, L.; Lietti, L. *Catal. Today* **2016,** *277*, 161. doi: 10.1016/j.cattod.2016.04.010

(79) Ngantsoue, H. W.; Zhang, Y. Q.; O'Brien, R. J.; Luo, M. S.; Davis, B. H. *Appl. Catal. A-Gen.* **2002,** *236*, 77. doi: 10.1016/S0926-860x(02)00278-8

(80) Martinelli, M.; Visconti, C. G.; Lietti, L.; Forzatti, P.; Bassano, C.; Deiana, P. *Catal. Today* **2014,** *228*, 77. doi: 10.1016/j.cattod.2013.11.018

(81) Satthawong, R.; Koizumi, N.; Song, C. S.; Prasassarakich, P. *Top Catal.* **2014,** *57*, 588. doi: 10.1007/s11244-013-0215-y

(82) Li, J. W.; Ding, Y. J.; Li, X. M.; Jiao, G. P.; Wang, T.; Chen, W. M.; Luo, H. Y. *Chem. Commun.* **2008,** *45*, 5954. doi: 10.1039/b813641f

(83) Chun, D. H.; Park, J. C.; Hong, S. Y.; Lim, J. T.; Kim, C. S.; Lee, H. T.; Yang, J. I.; Hong, S.; Jung, H. *J. Catal.* **2014,** *317*, 135. doi: 10.1016/j.jcat.2014.06.014

(84) Willauer, H. D.; Ananth, R.; Olsen, M. T.; Drab, D. M.; Hardy, D. R.; Williams, F. W. *J. CO_2 Util.* **2013,** *3–4*, 56. doi: 10.1016/j.jcou.2013.10.003

(85) Foraita, S.; Fulton, J. L.; Chase, Z. A.; Vjunov, A.; Xu, P. H.; Barath, E.; Camaioni, D. M.; Zhao, C.; Lercher, J. A. *Chem-Eur. J.* **2015,** *21*, 2423. doi: 10.1002/chem.201405312

(86) Kiatphuengporn, S.; Jantaratana, P.; Limtrakul, J.; Chareonpanich, M. *Chem. Eng. J.* **2016,** *306*, 866. doi: 10.1016/j.cej.2016.08.029

(87) Minett, D. R.; O'Byrne, J. P.; Pascu, S. I.; Plucinski, P. K.; Owen, R. E.; Jones, M. D.; Mattia, D. *Catal. Sci. Technol.* **2014,** *4*, 3351. doi: 10.1039/c4cy00616j

(88) Zhong, L. S.; Yu, F.; An, Y. L.; Zhao, Y. H.; Sun, Y. H.; Li, Z. J.; Lin, T. J.; Lin, Y. J.; Qi, X. Z.; Dai, Y. Y.; *et al*. *Nature* **2016,** *538*, 84. doi: 10.1038/nature19786

(89) Zhang, Y. Q.; Gary, J.; Dennis, E. S.; Mark, E. D.; Burtron, H. D. *Catal. Today* **2002,** *71*, 411. doi: 10.1016/S0920-5861(01)00468-0

(90) Thomas, R.; Michael, C.; Hans, S.; Georg, S.; Sang, S. N.; Jun, K. W.; Choi, M. J.; Gurram, K.; Lee, K. W. *Appl. Catal. A-Gen.* **1999,** *186*, 201. doi: 10.1016/S0926-860X(99)00173-8

(91) Mattia, D.; Jones, M. D.; P., J.; Griffiths, O. G.; Owen, R. E.; Sackville, E.; Mcmanus, M. *ChemSusChem* **2015,** *8*, 4064. doi: 10.1002/cssc.201500739

(92) Chakrabarti, D.; de Klerk, A.; Prasad, V.; Gnanamani, M. K.; Shafer, W. D.; Jacobs, G.; Sparks, D. E.; Davis, B. H. *Ind. Eng. Chem. Res.* **2015,** *54*, 1189. doi:10.1021/ie503496m

(93) Li, C. M.; Ban, H. Y.; Cai, W. J.; Zhang, Y.; Li, Z.; Fujimoto, K. *J. Saudi. Chem. Soc.* **2017,** *21*, 974. doi: 10.1016/j.jscs.2017.05.003

(94) Kattel, S.; Ramirez, P. J.; Chen, J. G.; Rodriguez, J. A.; Liu, P. *Science* **2017,** *355*, 1296. doi: 10.1126/science.aal3573

(95) Li, M. M. J.; Zeng, Z. Y.; Liao, F. L.; Hong, X. L.; Tsang, S. C. E. *J. Catal.* **2016,** *343*, 157. doi: 10.1016/j.jcat.2016.03.020

(96) Larmier, K.; Liao, W. C.; Tada, S.; Lam, E.; Verel, R.; Bansode, A.; Urakawa, A.; Comas-Vives, A.; Coperet, C. *Angew. Chem. Int. Edit.* **2017,** *56*, 2318. doi: 10.1002/anie.201610166

(97) Liao, F. L.; Wu, X. P.; Zheng, J. W.; Li, M. M. J.; Kroner, A.; Zeng, Z. Y.; Hong, X. L.; Yuan, Y. Z.; Gong, X. Q.; Tsang, S. C. E. *Green Chem.* **2017,** *19*, 270. doi: 10.1039/c6gc02366e

(98) Bai, S. X.; Shao, Q.; Feng, Y. G.; Bu, L. Z.; Huang, X. Q. *Small* **2017,** *13*, 1604311. doi: 10.1002/Smll.201604311

(99) Posada-Perez, S.; Ramirez, P. J.; Evans, J.; Vines, F.; Liu, P.; Illas, F.; Rodriguez, J. A. *J. Am. Chem. Soc.* **2016,** *138*, 8269. doi: 10.1021/jacs.6b04529

(100) Tada, S.; Watanabe, F.; Kiyota, K.; Shimoda, N.; Hayashi, R.; Takahashi, M.; Nariyuki, A.; Igarashi, A.; Satokawa, S. *J. Catal.* **2017,** *351*, 107. doi: 10.1016/j.jcat.2017.04.021

(101) Fujiwara, M.; Satake, T.; Shiokawa, K.; Sakurai, H. *Appl. Catal. B-Environ.* **2015,** *179*, 37. doi: 10.1016/j.apcatb.2015.05.004

(102) Saeidi, S.; Amin, N. S.; Rahimpour, M. R. *J. CO_2 Util.* **2014,** *5*, 66. doi: 10.1016/j.jcou.2013.12.005

(103) Wang, J. J.; You, Z. Y.; Zhang, Q. H.; Deng, W. P.; Wang, Y. *Catal. Today* **2013,** *215*, 186. doi: 10.1016/j.cattod.2013.03.031

(104) Visconti, C. G.; Martinelli, M.; Falbo, L.; Infantes-Molina, A.; Lietti, L.; Forzatti, P.; Iaquaniello, G.; Palo, E.; Picutti, B.; Brignoli, F. *Appl. Catal. B-Environ.* **2017,** *200*, 530. doi: 10.1016/j.apcatb.2016.07.047

(105) Wei, J.; Sun, J.; Wen, Z. Y.; Fang, C. Y.; Ge, Q. J.; Xu, H. Y. *Catal. Sci. Technol.* **2016,** *6*, 4786. doi: 10.1039/c6cy00160b

(106) Owen, R. E.; O'Byrne, J. P.; Mattia, D.; Plucinski, P.; Pascu, S. I.; Jones, M. D. *ChemPlusChem* **2013,** *78*, 1536. doi: 10.1002/cplu.201300263

(107) Wang, C. X.; Wang, X. B. *Adv. Mater. Res-Switz* **2012,** *347-353*, 808. doi: 10.4028/www.scientific.net/AMR.347-353.808

(108) Gupta, S.; Jain, V. K.; Jagadeesan, D. *ChemNanoMat* **2016,** *2*, 989. doi: 10.1002/cnma.201600234

(109) Yang, L.; Li, J.; Cao, J. X. *Appl. Mech. Mater.* **2013,** *423–426*, 463. doi: 10.4028/www.scientific.net/AMM.423-426.463

(110) Hu, S.; Liu, M.; Ding, F. S.; Song, C. S.; Zhang, G. L.; Guo, X. W. *J. CO_2 Util.* **2016,** *15*, 89. doi: 10.1016/j.jcou.2016.02.009

(111) Gao, J. J.; Jia, C. M.; Liu, B. *Catal. Sci. Technol.* **2017,** *7*, 5602. doi: 10.1039/C7CY01549F

(112) Zhang, J. L.; Lu, S. P.; Su, X. J.; Fan, S. B.; Ma, Q. X.; Zhao, T. S. *J. CO_2 Util.* **2015,** *12*, 95. doi: 10.1016/j.jcou.2015.05.004

(113) Numpilai, T.; Witoon, T.; Chanlek, N.; Limphirat, W.; Bonura, G.; Chareonpanich, M.; Limtrakul, J. *Appl. Catal. A-Gen.* **2017,** *547*, 219. doi:10.1016/j.apcata.2017.09.006

(114) Meiri, N.; Dinburg, Y.; Amoyal, M.; Koukouliev, V.; Nehemya, R. V.; Landau, M. V.; Herskowitz, M. *Faraday Discuss.* **2015,** *183*, 197. doi: 10.1039/c5fd00039d

(115) Satthawong, R.; Koizumi, N.; Song, C. S.; Prasassarakich, P. *Catal. Today* **2015,** *251*, 34. doi: 10.1016/j.cattod.2015.01.011

(116) Numpilai, T.; Witoon, T.; Chanlek, N.; Limphirat, W.; Bonura, G.; Chareonpanich, M.; Limtrakul, J. *Appl. Catal. A-Gen.* **2017,** *547*, 219. doi: 10.1016/j.apcata.2017.09.006

(117) Van Santen, R. A.; Ciobîcă, I. M.; Van Steen, E.; Ghouri, M. M. *Advances in Catalysis*; Gates, B. C., Knözinger, H., Eds.; Elsevier Science & Technology: Salt Lake City,USA, 2011; Vol. 54, p 127.

(118) Owen, R. E.; Mattia, D.; Plucinski, P.; Jones, M. D. *ChemPhysChem* **2017,** *18*, 3211. doi: 10.1002/cphc.201700422

(119) Newsome, D. S. *Catal. Rev.* **2006,** *21*, 275. doi: 10.1080/03602458008067535

(120) Van, D. L.; Gerard, P.; Beenackers, A. A. C. M. *Catal. Rev.* **1999,** *41*, 255. doi: 10.1081/CR-100101170

(121) You, Z. Y.; Deng, W. P.; Zhang, Q. H.; Wang, Y. *Chinese J. Catal.* **2013,** *34*, 956. doi: 10.1016/S1872-2067(12)60559-2

(122) Cheng, K. S.; Ordomsky, V. V.; Legras, B.; Virginie, M.; Paul, S.; Wang, Y.; Khodakov, A. Y. *Appl. Catal. A-Gen.* **2015,** *502*, 204. doi: 10.1016/j.apcata.2015.06.010

(123) Ye, J. Y.; Liu, C. J.; Ge, Q. *J. Phys. Chem. C* **2012,** *116*, 7817. doi: 10.1021/jp3004773

(124) Chen, M.; Xu, J.; Liu, Y. M.; Cao, Y.; He, H. Y.; Zhuang, J. H. *Appl. Catal. A-Gen.* **2010,** *377*, 35. doi: 10.1016/j.apcata.2010.01.011

(125) Hu, B. X.; Frueh, S.; Garces, H. F.; Zhang, L. C.; Aindow, M.; Brooks, C.; Kreidler, E.; Suib, S. L. *Appl. Catal. B-Environ.* **2013,** *132*, 54. doi: 10.1016/j.apcatb.2012.11.003

(126) Lee, J. F.; Chern, W. S.; Lee, M. D.; Dong, T. Y. *Can. J. Chem. Eng.* **1992,** *70*, 511. doi: 10.1002/cjce.5450700314

(127) Dorner, R. W.; Hardy, D. R.; Williams, F. W.; Willauer, H. D. *Catal. Commun.* **2011,** *15*, 88. doi: 10.1016/j.catcom.2011.08.017

(128) Prasad, P. S. S.; Bae, J. W.; Jun, K. W.; Lee, K. W. *Catal. Surv. Asia* **2008,** *12*, 170. doi: 10.1007/s10563-008-9049-1

(129) Falbo, L.; Martinelli, M.; Visconti, C. G.; Lietti, L.; Forzatti, P.; Bassano, C.; Deiana, P. *Ind. Eng. Chem. Res.* **2017,** *56*, 13147. doi: 10.1021/acs.iecr.7b01494

(130) Zhang, J.; Lu, S.; Su, X.; Fan, S.; Ma, Q.; Zhao, T. *J. CO_2 Util.* **2015,** *12*, 95. doi: 10.1016/j.jcou.2015.05.004

(131) Chen, W.; Fan, Z. L.; Pan, X. L.; Bao, X. H. *J. Am. Chem. Soc.* **2008,** *130*, 9414. doi: 10.1021/ja8008192

(132) Liu, X. L.; Wang, M. H.; Zhou, C.; Zhou, W.; Cheng, K.; Kang, J. C.; Zhang, Q. H.; Deng, W. P.; Wang, Y. *Chem. Commun.* **2018,** *54*, 140. doi: 10.1039/c7cc08642c

(133) Spivey, J. J.; Egbebi, A. *Chem. Soc. Rev.* **2007,** *36*, 1514. doi: 10.1039/b414039g

(134) He, Z. H.; Qian, Q. L.; Ma, J.; Meng, Q. L.; Zhou, H. C.; Song, J. L.; Liu, Z. M.; Han, B. X. *Angew. Chem.-Int. Edit.* **2016,** *55*, 737. doi: 10.1002/anie.201507585

(135) Chen, Y.; Choi, S. M.; Thompson, L. T. *J. Catal.* **2016,** *343*, 147. doi: 10.1016/j.jcat.2016.01.016

(136) Cui, M.; Qian, Q. L.; He, Z. H.; Zhang, Z. F.; Ma, J.; Wu, T. B.; Yang, G. Y.; Han, B. X. *Chem. Sci.* **2016,** *7*, 5200. doi: 10.1039/c6sc01314g

(137) Zhang, J. J.; Qian, Q. L.; Cui, M.; Chen, C. J.; Liu, S. S.; Han, B. X. *Green Chem.* **2017,** *19*, 4396. doi: 10.1039/c7gc01887h

(138) Qian, Q. L.; Cui, M.; Zhang, J. J.; Xiang, J. F.; Song, J. L.; Yang, G. Y.; Han, B. X. *Green Chem.* **2018,** *20*, 206. doi: 10.1039/c7gc02807e

(139) Guo, W.; Gao, W. G.; Wang, H.; Tian, J. J. *Sol. Energ. Mat. Sol. C.* **2014,** *827*, 20. doi: 10.4028/www.scientific.net/AMR.827.20

(140) Shang, G. L.; Hu, J. G.; Hai, R. Z.; Jun, L.; Lian, X.; Cai, R. L.; Xin, D. C. *Adv. Mater. Res.* **2013,** *772*, 275. doi: 10.4028/www.scientific.net/AMR.772.275

(141) Liu, S.; Zhou, H. B.; Song, Q. Y.; Ma, Z. *J. Taiwan Inst. Chem. E.* **2017,** *76*, 18. doi: 10.1016/j.jtice.2017.04.007

(142) Ouyang, B.; Xiong, S. H.; Zhang, Y. H.; Liu, B.; Li, J. L. *Appl. Catal. A-Gen.* **2017,** *543*, 189. doi: 10.1016/j.apcata.2017.06.031

(143) Kiatphuengporn, S.; Chareonpanich, M.; Limtrakul, J. *Chem. Eng. J.* **2014,** *240*, 527. doi: 10.1016/j.cej.2013.10.090

(144) Guo, H. J.; Li, S. G.; Peng, F.; Zhang, H. R.; Xiong, L.; Huang, C.; Wang, C.; Chen, X. D. *Catal. Lett.* **2015,** *145*, 620. doi: 10.1007/s10562-014-1446-7

(145) Okabe, K.; Yamada, H.; Hanaoka, T.; Matsuzaki, T.; Arakawa, H.; Abe, Y. *Chem. Lett.* **2001,** *30*, 904. doi: 10.1246/cl.2001.904

(146) Kusama, H.; Okabe, K.; Sayama, K.; Arakawa, H. *Appl. Organomet. Chem.* **2000,** *12*, 836. doi: 10.1002/1099-0739(200012)14:123.0.CO;2-C

(147) Kishida, M.; Yamada, K.; Nagata, H.; Wakabayashi, K. *Chem. Lett.* **1994,** *23*, 555. doi: 10.1246/cl.1994.555

(148) Inui, T.; Yamamoto, T.; Inoue, M.; Hara, H.; Takeguchi, T.; Kim, J. B. *Appl. Catal. A-Gen.* **1999,** *186*, 395. doi: 10.1016/S0926-860X(99)00157-X